ARTICLES

Resonant Vibrational Excitation and De-Excitation of CO(v) by Low Energy Electrons

G. B. Poparić,*,† M. Ristić,‡ and D. S. Belić†

Faculty of Physics, University of Belgrade, Studentski trg 12, P.O. Box 368, 11000 Belgrade, Serbia, and Faculty of Physical Chemistry, University of Belgrade, Studentski trg 12, P.O. Box 137, 11000 Belgrade, Serbia

Received: June 22, 2008; Revised Manuscript Received: October 5, 2008

Integral cross sections and rate coefficients for vibrational excitation of the excited carbon-monoxide molecule, via the $^2\Pi$ shape resonance in the energy region from 0 to 5 eV have been calculated. Cross sections are calculated by using our recently measured cross sections for the ground level CO excitation and the most recent cross sections for elastic electron scattering, applying the principle of detailed balance. Rate coefficients are calculated for Maxwellian electron energy distribution, with mean electron energies below 5 eV. By using extended Monte Carlo simulations, electron energy distribution functions (EEDF) and rate coefficients are determined in nonequilibrium conditions, in the presence of homogeneous external electric field. Nonequilibrium rates are calculated for typical, moderate values of the electric field over gas number density ratios, E/N, from 1 to 220 Td. Maxwellian and nonequilibrium rate coefficients are compared and the difference is attributed to a specific shape of the electron energy distribution functions under considered conditions.

Introduction

Electron collision processes with carbon-monoxide are important in plasma and discharge technology, ionized gases, chemical detectors and in laser devices.[1,2] For modeling all of these phenomena, one needs to know cross sections and rates for various involved processes. At low electron energies, vibrational excitation is dominant process of energy transfer. In order to determine rate coefficients for these processes it is necessary to have accurate absolute differential cross sections, both for vibrational excitation and elastic scattering as a function of energy as well as their angular distributions.

Vibrational excitation of the ground-state of CO molecule by electron impact has been intensively investigated.[3,4] Significant resonant contribution of the $^2\Pi$ shape resonance to this process, with the maximum around 2 eV, was first observed by Schulz[5] and Ehrhardt et al.[6] This phenomenon was successfully described by the boomerang model, introduced by Birtwistle and Herzenberg.[7]

Relative differential cross sections (DCS) as a function of incident energy, in the energy region from 0.6 to 5 eV, and angular distributions of inelastically scattered electrons by CO have been measured by Ehrhardt et al.[6] for the excitation of $v = 1$ to 7 vibrational levels and by Jung et al.[8] for the resolved rotational excitation. Angular distributions are measured from 5 to 110°. Middleton et al.[9] and Gibson et al.[10] have also reported DCS for vibrational excitation for energies between 1 and 50 eV and for scattering angles up to 130°. More recently, Poparić et al.[11] have measured the ratio of DCS at 0 and 180°, by use of a time-of-flight technique.

Theoretical calculations have been performed in Born dipole approximation (BDA) by Sohn et al.,[12] R-matrix calculations by Morgan and Tennyson[13] and by Morgan.[10] It has been pointed out by Brunger and Buckman[4] that, near the $^2\Pi$ resonance maximum, experimental data agree with each other fairly well and generally are well reproduced by the theory.

Integral cross sections (ICS) for excitation of the first vibrational level ($v = 0 \rightarrow 1$) of CO have been reported by Land,[14] as a result of swarm experiments, by Sohn et al.,[12] by Chutjian and Tanaka,[15] and by Gibson et al..[10] Normalized ICS for excitation of the lower 10 vibrational levels are reported recently by Poparić et al.[16] Theoretical calculations of ICS are performed by Morgan[10] and Morgan and Tennyson,[13] using R-matrix formalism and BDA. A good overall agreement has been achieved between theory and experiment.

Rate coefficients for vibrational excitation of CO have been calculated by Ristić et al.,[17] for Maxwellian electron energy distribution function and for nonequilibrium conditions by using Monte Carlo simulation technique. Electron energy transfer rates for vibrational excitation of CO in the atmospheres of Mars and Venus have been calculated recently by Campbell and Brunger[18] and compared to the rates for CO_2.

The aim of this paper is to obtain partial and total rate coefficients for excitation of vibrationaly excited CO(v) below and in the $^2\Pi$ resonance region. ICS for excited levels are determined by using our recently measured cross sections for ground level CO excitation[16] and the most recent cross sections for elastic electron scattering, applying the principle of detailed balance. Rate coefficients are calculated for Maxwellian electron energy distribution, for the mean electron energies below 5 eV. By using extended Monte Carlo simulations, electron energy distribution functions (EEDF) and rate coefficients are determined in nonequilibrium conditions.

* To whom correspondence should be addressed. E-mail: Goran_Poparic@ff.bg.ac.yu.
† Faculty of Physics.
‡ Faculty of Physical Chemistry.

10.1021/jp8054922 CCC: $40.75
Published on Web 10/31/2008

Vibrational Excitation Cross Sections of CO(v)

Low energy electron impact vibrational excitation cross sections of CO were measured[16] by use of a high resolution crossed-beams double trochoidal electron spectrometer.[19,20] Excitation functions from $v = 0$ of CO ground-state to the first 10 vibrationally excited states ($v = 1$ to 10) via the $^2\Pi$ resonance were measured.[16] These are in fact relative differential cross sections for electrons scattered in forward and backward directions. Contributions from 0 and 180° are separated using time-of-flight technique. This ratio is found to be 1.00 ± 0.05 for all vibrational levels.

Theoretical predictions for angular distribution of scattered electrons proposed by Read[21] for heteronuclear diatomic molecules are used to normalize our results to the Gibson et al.[10] data. Type I resonance (Read)[21] is considered with contributions of pπ and dπ waves. Theoretically proposed expression with two fitting parameters is used to fit the data of Gibson et al.,[10] from 15 to 130°, with our results of equal values at 0 and 180°. Absolute DCS values at 0 and at 180° are found to be $(7.4 \pm 0.9) \times 10^{-17}$ cm^2 sr^{-1}. DCS for all other vibrational levels are normalized by using their relative count rate under the same experimental conditions (gas pressure, electron beam current, residual electron energy, and signal accumulation time).

The ratios of the particular DCS at the maximum relative to the DCS for $v = 1$ are compared with the results of relative measurements obtained by Allan,[22] and these are found to be lower, for all vibrational levels. The data of Ehrhardt et al.[6] are in better agreement with our data, especially for the first five vibrational levels.

By using the results of our fitting procedure, integral cross sections for electron impact excitation of the first 10 vibrational levels of CO are obtained. Corresponding ICSs for excitation from vibrationaly excited levels of CO(v) and for de-excitation processes to lower vibrational levels are determined from our measured data set[16] by using the principle of detailed balance (Fowler 1936;[23] Mihajlov et al. 1999;[24] and Campbell et al. 2004)[25] and the elastic cross sections of Gibson el al.[10] Cross section for electron impact transition from the initial level v to the final level k is given by[24]

$$\sigma_{vk}(\varepsilon) = \frac{(\varepsilon + \varepsilon_v)}{\varepsilon} \frac{\sigma_{0v}(\varepsilon + \varepsilon_v)\sigma_{0k}(\varepsilon + \varepsilon_v)}{\sigma_{00}(\varepsilon + \varepsilon_v)} \qquad (1)$$

Here, σ_{00} is the resonant part of the ground level elastic cross section, σ_{0v} and σ_{0k} are the inelastic cross sections for vibrational excitation of the levels v and k from the ground-state, and ε and ε_v are the electron energy and the energy of the initial level v, respectively.

We have determined ICSs for inelastic, elastic and superelastic transitions between all levels with $v, k \leq 5$. The results are shown in Figure 1. For each cross section, corresponding transition is indicated in the figure. With $v = k$ elastic processes are indicated, with $v < k$ inelastic and with $v > k$ superelastic processes are shown. It should be noted that the vertical scale is different and that the cross sections decrease rapidly with increasing v or k, or both of them.

In performing cross section and rate coefficient calculations, important role have resonance threshold energies for corresponding transitions. A great care has been dedicated to this issue. These thresholds are determined as a difference between the initial energy level and beginning of the resonance. The latter is determined accurately from our experimental results for ground level excitation functions, Poparić et al.,[16] for all vibrational levels. Determined threshold energies are listed in Table 1. For each transition between initial level v and final level k threshold energy is indicated in the table in eV.

Results and Discussion

Rate coefficients for vibrational excitation and de-excitation of *CO*(v) are determined by using our set of integral cross sections introduced in section 2. Calculations are performed both for Maxwellian and nonequilibrium electron energy distribution functions (EEDF). For Maxwellian EEDF rate coefficients are determined for a number of mean electron energy values in the range from 0 to 5 eV. Vibrational rate coefficients in the nonequilibrium case, in a presence of homogeneous external electric field, are determined by extended Monte Carlo simulation technique, for moderate values of the field strength and gas number density ratios, *E*/*N*.

Maxwellian EEDF rate coefficients. The rate coefficient, *K*, for vibrational excitation is given by[26,27]

$$K(\bar{E}_{el}) = \sqrt{2/m_e} \int_{\varepsilon_{thres}}^{+\infty} \sigma_v(\varepsilon) \sqrt{\varepsilon} f_e(\bar{E}_{el}, \varepsilon)\, d\varepsilon \qquad (2)$$

where $\bar{E}_{el}$ is the mean electron energy, $\sigma_v(\varepsilon)$ is the vibrational excitation cross section and $f_e(\bar{E}_{el}, \varepsilon)$ is the normalized electron energy distribution function

$$\int_0^{+\infty} f_e(\bar{E}_{el}, \varepsilon)\, d\varepsilon = 1 \qquad (3)$$

For the equilibrium case, the electron energy distribution function is given by the Maxwellian equation

$$f_e(\bar{E}_{el}, \varepsilon) = 2\pi^{-1/2}(3/2\bar{E}_{el})^{+3/2} \sqrt{\varepsilon} \exp(-3\varepsilon/2\bar{E}_{el}) \qquad (4)$$

For this case the rate coefficients are determined by the direct numerical integration of our integral cross section data. The rate coefficients are calculated for all vibrational transitions between vibrational levels $0 \leq v, k \leq 5$ including inelastic, elastic and superelastic processes. Obtained results are shown in Figure 2. Calculations are performed for the mean electron energies up to 5 eV. The rate coefficients from $v = 0$ are also shown in the figure, for comparison. The last ones are calculated earlier by Ristić et al.,[17] but here only the resonant part of the ICS is included and consequently present rates from $v = 0$ are lower than in,[17] in particular for ($v = 0 \rightarrow 1$) transition.

The rate coefficients are arranged by the initial vibrational level. For each transition initial level v and final level k are indicated in the figure. The maxima of the rate coefficients range from 10^{-8} to 10^{-11} cm^3 s^{-1} and most of them are situated at the mean electron energies between 1 and 2 eV. It can be seen from the figure that for $v = 5$, for lower values of final quantum number k, rate coefficients have pronounced hump on the low energy side. This is the result of the low threshold energy for those cross sections, as can be seen from the Table 1.

In order to illustrate relative magnitudes of the coefficients we have shown corresponding values of the maxima for all transitions with $0 \leq v, k \leq 5$ in a 3D plot in Figure 3. The rate coefficients for mean electron energy of 1.6 eV are plotted versus initial and final vibrational quantum numbers which define corresponding transitions. As it can be noted, the vertical axis is logarithmic and thus the rate coefficients decrease rapidly with increasing one or both quantum numbers.

Valuable information can be drawn out by comparing rate coefficients for various processes regarding their classification from the point of view of transfer of energy between the electron and the target molecule in its excited states. In Figure 4, rate coefficients for superelastic, elastic, and inelastic processes are shown. They represent the sum of rates for transitions in which

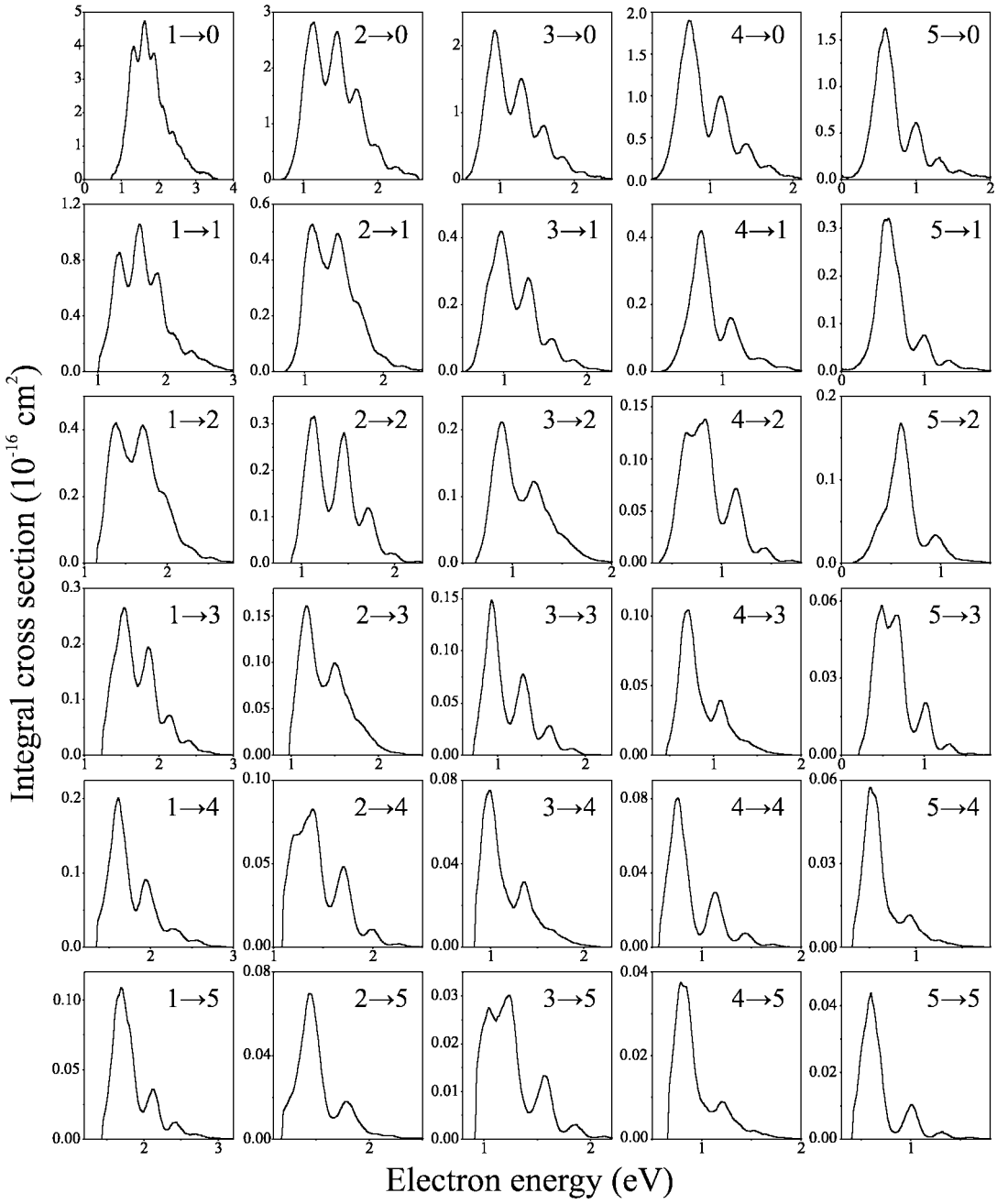

Figure 1. Integral cross sections for vibrational excitation and de-excitation of $CO(v)$ for $v, k \leq 5$.

TABLE 1: Resonance Threshold Energies for Vibrational Transitions in CO (in eV)

v/*k*	0	1	2	3	4	5
0	0.940	1.280	1.420	1.510	1.620	1.710
1	0.674	1.014	1.154	1.244	1.354	1.444
2	0.412	0.752	0.892	0.982	1.092	1.182
3	0.153	0.493	0.633	0.723	0.833	0.923
4		0.237	0.377	0.467	0.577	0.667
5			0.125	0.215	0.325	0.415

electrons gain energy, do not exchange energy or transfer a part of their kinetic energy to the excitation of the molecule to higher vibrational level, respectively. As it is depicted in Figure 1, inelastic cross sections are generally lower than elastic and superelastic and that causes the total inelastic rate coefficient to be lower than other two, especially at low mean electron energies where thresholds for inelastic processes have not yet been reached. Although most of superelastic ICSs are higher than elastic and although the number of superelastic processes is higher than elastic, the total superelastic rate coefficient dominates elastic only at low mean electron energies (below 0.5 eV) where thresholds for superelastic processes are reached. The reason is very high ICS for $v = 0$ to $k = 0$ resonant transition, with threshold at 0.94 eV, which is more than ten times higher from the ICS for $1 \rightarrow 1$ and other elastic transitions. The total elastic rate coefficient rises with mean electron energy and reaches maximum at 2.2 eV of mean electron energy, where it overwhelms the total superelastic rate coefficient by almost a factor of 3.

Nonequilibrium EEDF Rate Coefficients. In order to determine the rate coefficients in the case of nonequilibrium conditions we have developed an extended Monte Carlo simulation technique.[28] We have simulated the movement of electrons through the *CO* gas in a presence of the uniform electric field. All scattering processes, both elastic and inelastic

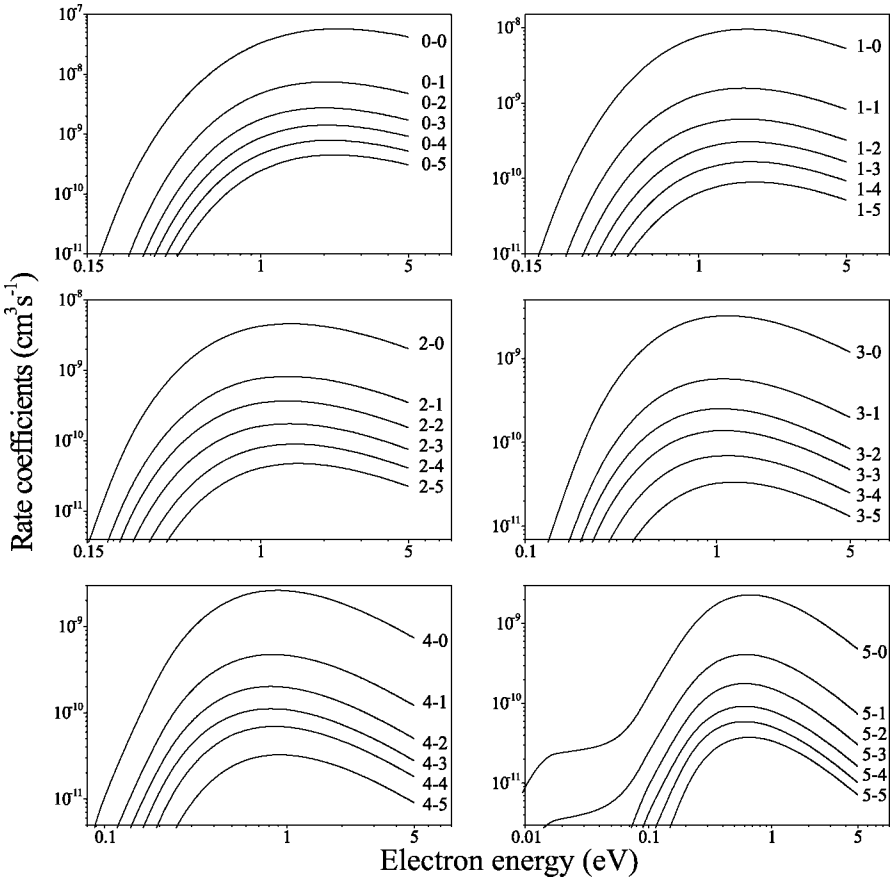

Figure 2. Vibrational excitation and de-excitation rate coefficients of CO(v) for Maxwellian EEDF. Initial and final states for each transition are indicated, $v \rightarrow k$.

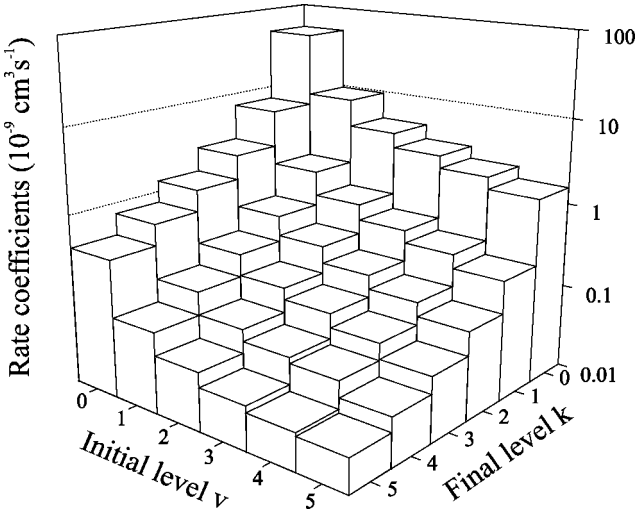

Figure 3. Vibrational excitation and de-excitation rate coefficients of *CO*(v) for Maxwellian EEDF at electron energy of 1.6 eV.

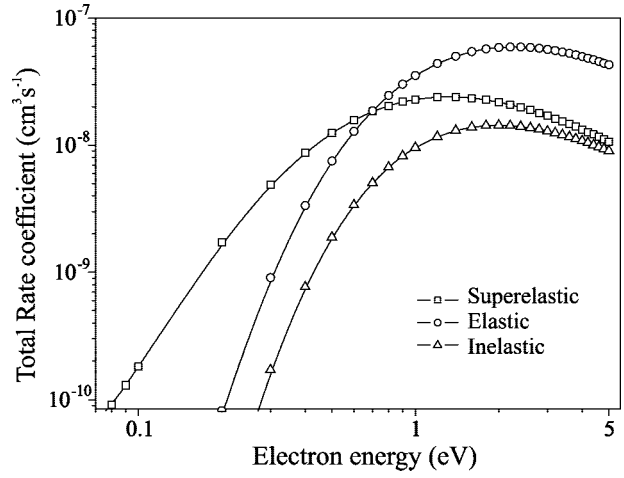

Figure 4. Comparison of total rate coefficients for superelastic (squares), elastic (circles) and inelastic (triangles) processes for equilibrium conditions.

are included in this modeling by using experimentally measured data of integral cross sections as a function of energy. The probability for possible elastic scattering, vibrational excitation, electronic excitation or ionization is proportional to the value of the corresponding integral cross sections. The decision of which possible processes will happen in each collision event is left to the pseudorandom generated numbers. The scattering angle of electrons after the collision is determined by using experimentally measured differential cross sections, i.e. corresponding angular distributions. In that way, the scattering angle is also determined by using pseudorandom numbers, but weighted by the real differential cross sections. Since the sets of integral and differential cross sections are measured for the discrete values of energy, we have dynamically interpolated all cross sections data for actual values of electron energy during its motion. This type of simulation is similar to the simulations developed earlier by White et al.[29] and by Stojanović et al.[30,31] In order to test our algorithm, we have used Reid ramp model gas[32] simulation tests. We have obtained the same results (within statistical error bars) for the mean electron energy and for the diffusion coefficients as White et al.[29] in their benchmark simulations.

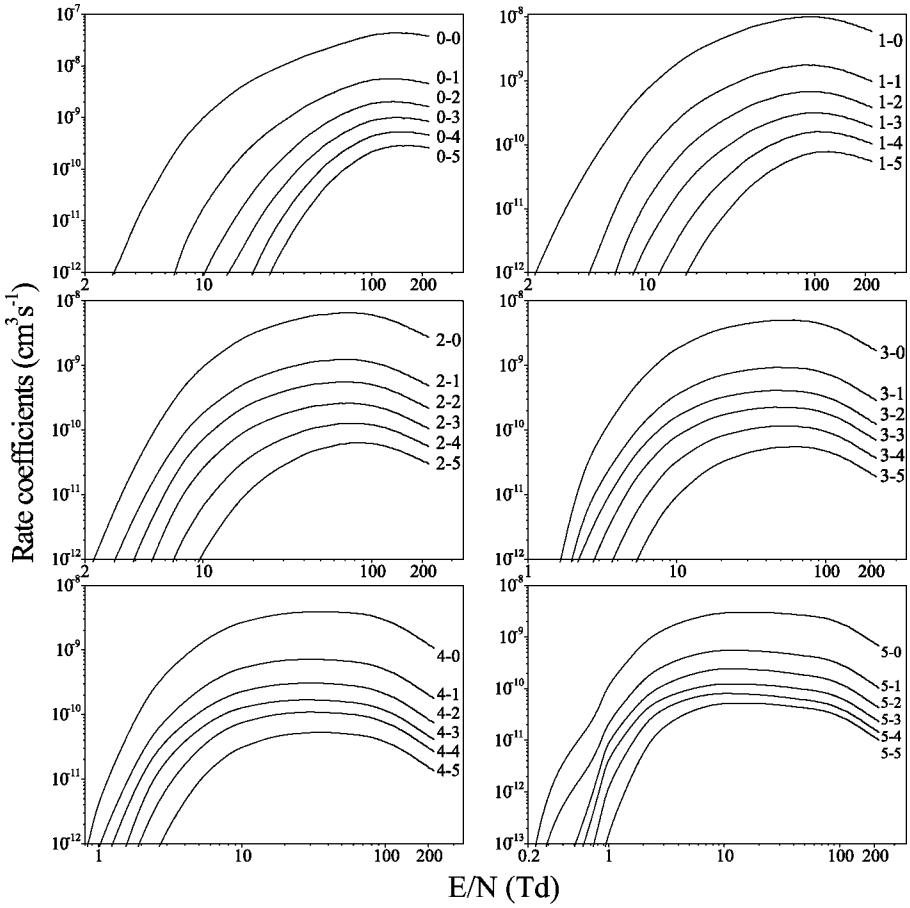

Figure 5. Nonequilibrium vibrational excitation and de-excitation rate coefficients for CO vs E/N value. Initial and final states for each transition are indicated.

For modeling electron diffusion through the carbon-monoxide gas, we have used the data for elastic scattering from other authors. In the energy range from zero to 10 eV, we have used the most recent data of Gibson et al.[10] For higher electron energies, from 10 to 75 eV, we have used the data of Gote and Ehrhardt.[33] Actually, only a small number of electrons reach energies higher than 20 eV in the case where the mean electron energy is in the range from zero to 5 eV, as is in our case. In modeling inelastic electron collision processes we used our experimentally measured and normalized integral cross section data for vibrational excitation, given in section 2 for energies from 0 to 10 eV and the data of Gibson et al.[10] and Chutjian and Tanaka[15] for higher energies. All other excitation processes of the valence and Rydberg levels of the CO molecule have lower cross sections and lie above 6 eV. Their contribution to electron scattering in the low energy region is estimated to be about 5% only. However these processes are included in the modeling. Included are also integral rotationally inelastic cross sections for ($J = 0 \rightarrow 1$) of Randall et al.[4,34] in the 2−100 meV energy region and those of Jung et al.[8] for ($J = 0 \rightarrow 1$) and ($J = 0 \rightarrow 2$) in the $^2\Pi$ resonance energy region. Integral cross sections for electron impact excitation of singlet electronic states of CO are included for $A^1\Pi$, $C^1\Sigma^+$, $E^1\Pi$, $I^1\Sigma^-$, and $D^1\Delta$ states from Liu and Victor[4,35] and for $B^1\Sigma^+$ state from Poparić.[36] Above 30 eV, more recent ICS for $A^1\Pi$ are used from Kato et al.[37] and for $C'^1\Sigma^+$ (together with $c^3\Pi$) and $E^1\Pi$ the data from Kawahara et al.[38] are used. For triplet electronic states we have included $a^3\Pi$ and $b^3\Sigma^+$ states from Poparić[36] and $a'^3\Sigma^+$, $d^3\Delta$, and $e^3\Sigma^-$ from Liu and Victor.[4,35] Also, integral cross sections for electron impact ionization of CO from Mangan et al.[39] are included in the modeling.

For the purpose of the nonequilibrium case calculations, by using Monte Carlo simulations for transport of electrons in the carbon-monoxide gas, we have generated electron energy distribution functions for different values of E/N, ranging from 0.1 to 220 Td, which corresponds to the mean electron energy values up to 5 eV. They are in a very good agreement with the data obtained by numerically solving Boltzmann equation based on the two term Legendre expansion of the velocity distribution function (Bolsig v1.05).[40,41] These EEDFs are used together with the vibrational excitation integral cross sections to calculate corresponding nonequilibrium rate coefficients. Obtained results for the partial vibrational excitation rate coefficients are shown in Figure 5.

The nonequilibrium rate coefficients also range from 10^{-8} to 10^{-11} cm^3 s^{-1}. They are arranged in the figure by the initial vibrational level. For each transition initial level v and final level k are indicated in the figure, $v \rightarrow k$. The rate coefficients from $v = 0$ are also shown in the figure for comparison. Same as in equilibrium case, only resonant part of the ICS is included and consequently present rates are lower than previously published by Ristić et al.,[17] in particular for the $0 \rightarrow 1$ transition. Relative magnitudes of the nonequilibrium coefficients decrease rapidly with the vibrational quantum numbers, similar as for Maxwellian case illustrated in Figure 2.

We have compared our results for excitation rates for the Maxwellian and for the nonequilibrium electron energy distributions, for inelastic transitions from nonground vibrational levels, in Table 2. The results from the ground vibrational level[17] are also included in the table. The comparison is made for the rate coefficients maxima, for E/N values in the nonequilibrium distribution which correspond to the same mean electron energy

TABLE 2: Rate Coefficients Maxima for $v-k$ Transitions for Maxwellian (Upper) and Non-Equilibrium (Lower Numbers) in 10^{-9} cm^3 s^{-1}

v/k	0	1	2	3	4	5
0	57.320	7.415	2.741	1.418	0.787	0.448
	43.785	5.717	2.052	1.009	0.535	0.290
1	9.536	1.577	0.615	0.306	0.167	0.090
	10.121	1.770	0.686	0.321	0.161	0.078
2	4.630	0.828	0.367	0.176	0.090	0.048
	6.573	1.239	0.558	0.262	0.129	0.065
3	3.255	0.577	0.252	0.138	0.070	0.034
	5.018	0.932	0.413	0.227	0.116	0.056
4	2.640	0.476	0.203	0.112	0.070	0.033
	3.904	0.717	0.306	0.168	0.108	0.052
5	2.286	0.413	0.178	0.093	0.060	0.038
	3.037	0.554	0.243	0.124	0.081	0.053

value in the Maxwellian distribution. The Maxwellian rates are presented with the top values and nonequilibrium with the bottom values. Maxwellian rates are higher for transitions from ground level and for $1 \rightarrow 4$ and $1 \rightarrow 5$ transitions. For all other transitions from excited vibrational levels, the nonequilibrium rates are significantly higher. This situation is expected having in mind EEDFs used to obtain these two sets of data.

The total rate coefficients for various processes, regarding their classification from the point of view of the transfer of energy between the electron and the target molecule in its excited states, are compared also for nonequilibrium conditions, in Figure 6. The total rate coefficients for the superelastic, elastic, and inelastic processes are shown. The total rate coefficient for the inelastic transitions is significantly lower in the whole region than both total elastic and total superelastic rate coefficient. This is the consequence of lower inelastic ICSs values. Although most of superelastic ICSs are higher than elastic and although the number of superelastic processes is higher than elastic, the total superelastic rate coefficient dominates elastic only at low mean electron energies (below 70 Td) where thresholds for superelastic processes are reached. As it is explained in section 3.1, the reason is very high ICS for $v = 0$ to $k = 0$ resonant transition, with threshold at 0.94 eV, which is more than ten times higher from the ICS for $1 \rightarrow 1$ and other elastic transitions. The total elastic rate coefficient rises with E/N ratio and reaches maximum at 140 Td, being two times higher than the total superelastic rate.

The total rate coefficients for Maxwellian and nonequilibrium conditions are shown together in Figure 7. The total rates for superelastic, elastic, and inelastic excitations, as presented in Figures 4 and 6, are compared with each other in this figure. The nonequilibrium rate coefficients are plotted versus mean electron energies obtained in simulations for corresponding E/N values.

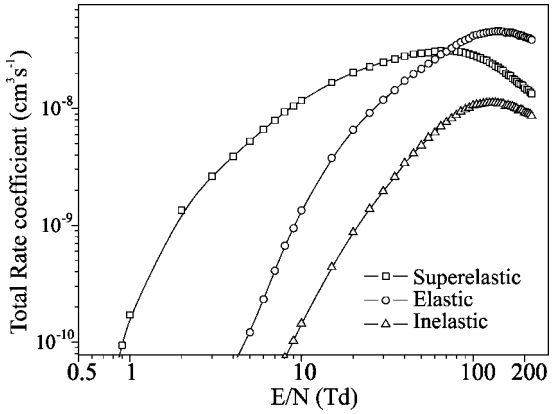

Figure 6. Comparison of total rate coefficients for superelastic (squares), elastic (circles), and inelastic (triangles) processes for nonequilibrium conditions.

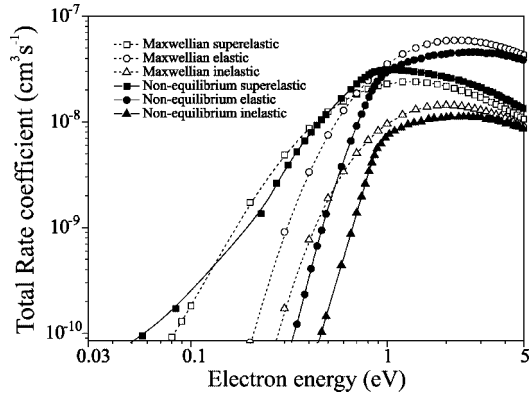

Figure 7. Total vibrational excitation rate coefficients for CO(v) for Maxwellian (dashed lines) and nonequilibrium (solid lines) EEDFs.

The total Maxwellian rate coefficients for elastic and inelastic processes are higher than nonequilibrium rate coefficients, which is expected having in mind that nonequilibrium EEDFs are narrower and shifted toward lower energies, comparing to Maxwellian EEDFs with the same mean electron energy. This is not the situation in the case of total superelastic rate coefficients, because of the low threshold energies for superelastic processes. At higher energies the Maxwellian and nonequilibrium rate coefficients approach each other.

Conclusions

Electron impact vibrational excitation of the CO molecule, via the $^2\Pi$ shape resonance, in the low electron energy region has been investigated. The cross sections for ground vibrational level excitation are used, by applying the principle of detailed balance, to obtain integral cross sections for transitions from vibrationaly excited levels CO(v). ICS for excitation, for elastic collisions and for de-excitation processes to lower vibrational levels are determined. ICSs for transitions between vibrational levels lower than 5 are determined. The rate coefficients for vibrational transitions are determined in equilibrium conditions with the Maxwellian electron energy distribution functions. The nonequilibrium electron energy distribution functions and rate coefficients are determined in the presence of homogeneous electric field for the moderate values of the field strength over gas number density ratios. The two sets of rate coefficients are compared with each other.

Acknowledgment. This work was supported in part by the Ministry of Science and Technological Development of the Republic of Serbia by the Project No. 141015.

References and Notes

(1) Hahn, J.; Junge, C. *Z. Naturforsch.* **1977**, *32a*, 190.
(2) Pearson, G. N.; Hall, D. R. *J. Phys. D: Appl. Phys.* **1989**, *22* (8), 1102–1106.
(3) Schulz, G. J. *Rev. Mod. Phys.* **1973**, *45* (3), 423–486.
(4) Brunger, M. J.; Buckman, S. J. *Phys. Rep.* **2002**, *357* (3−5), 215–458.
(5) Schulz, G. J. *Phys. Rev.* **1964**, *135* (4A), A988–A994.
(6) Ehrhardt, H.; Langhans, L.; Linder, F.; Taylor, H. S. *Phys. Rev.* **1968**, *173* (1), 222–230.
(7) Birtwistle, D. T.; Herzenberg, A. *J. Phys. B: At. Mol. Phys.* **1971**, *4* (1), 53–70.
(8) Jung, K.; Antoni, T.; Muller, R.; Kochem, K.-H.; Ehrhardt, H. *J. Phys. B: At. Mol. Phys.* **1982**, *15* (19), 3535–3555.

(9) Middleton, A. G.; Brunger, M. J.; Teubner, P. J. O. *J. Phys. B: At. Mol. Phys.* **1992**, *25* (16), 3541–3549.
(10) Gibson, J. C.; Morgan, L. A.; Gulley, R. J.; Brunger, M. J.; Bundschu, C. T.; Buckman, S. J. *J. Phys. B: At. Mol. Phys.* **1996**, *29* (14), 3197–1395.
(11) Poparić, G. B.; Galijas, S. M. D.; Belić, D. S *Phys. Rev. A.* **2004**, *70* (2), 024701.
(12) Sohn, W.; Kochem, K.-H.; Jung, K.; Ehrhardt, H.; Chang, E. S. *J. Phys. B: At. Mol. Phys.* **1985**, *18* (10), 2049–2055.
(13) Morgan, L. A.; Tennyson, J. *J. Phys. B: At. Mol. Phys.* **1993**, *26* (15), 2429–2441.
(14) Land, J. E. *J. Appl. Phys.* **1978**, *49*, 5716.
(15) Chutjian, A.; Tanaka, H. *J. Phys. B: At. Mol. Phys.* **1980**, *13* (9), 1901–1908.
(16) Poparić, G. B.; Belić, D. S.; Vićić, M. D *Phys. Rev. A.* **2006**, *73*, 062713.
(17) Ristić, M.; Poparić, G. B.; Belić, D. S. *Chem. Phys.* **2007**, *336* (1), 58–63.
(18) Campbell, L.; Brunger, M. J. *PMC Phys. B* **2008**, *1*, 3.
(19) Vićić, M. D.; Poparić, G. B.; Belić, D. S. *Rev. Sci. Instrum.* **1998**, *69* (5), 1996–1999.
(20) Poparić, G. B.; Vićić, M. D.; Belić, D. S. *Phys. Rev. A.* **2002**, *66* (2), 022711.
(21) Read, F. H. *J. Phys. B: At. Mol. Phys.* **1968**, *1*, 893–908.
(22) Allan, M. *J. Electron Spectrosc. Relat. Phenom.* **1989**, *48* (2), 219–351.
(23) Fowler, R. H. *Statistical Mechanics. The Theory of the Properties of Matter in Equilibrium*; The University Press: Cambridge, U.K., 1936.
(24) Mihajlov, A. A.; Stojanović, V. D.; Petrović, Z. L. *J. Phys. D: Appl. Phys.* **1999**, *32* (20), 2620–3629.
(25) Campbell, L.; Brunger, M. J.; Cartwright, D. C.; Teubner, P. J. O. *Planet. Space Sci.* **2004**, *52* (9), 815–822.
(26) Chantry P. Final Technical Report ARPA, Order No 3342; Harvard-Smithsonian Centre for Astrophysics, 1978.
(27) Belić, D. S. *Chem. Phys.* **1989**, *130* (1−3), 141.
(28) Ristić, M.; Poparić, G. B.; Belić, D. S. *Chem. Phys.* **2007**, *331* (2−3), 410–416.
(29) White, R. D.; Brennan, M. J.; Ness, K. F. *J. Phys. D: Appl. Phys.* **1997**, *30* (5), 810–816.
(30) Stojanović, V. D.; Jelenković, B.; Petrović, Z. L. *J. Appl. Phys.* **1997**, *81*, 1601.
(31) Stojanović, V. D.; Petrović, Z. L. *J. Phys. D: Appl. Phys.* **1998**, *31* (7), 834–846.
(32) Reid, I. D. *Aust J. Phys.* **1979**, *32*, 231–254.
(33) Gote, M.; Ehrhardt, H. *J. Phys. B: At. Mol. Phys.* **1995**, *28* (17), 3957–3986.
(34) Randell, J.; Gulley, R. J.; Lunt, S. L.; Ziesel, J. P.; Field, D. *J. Phys. B: At. Mol. Phys.* **1996**, *29* (10), 2049–2058.
(35) Liu, W.; Victor, G. A. Report Series No. 3872; Harvard-Smithsonian Centre for Astrophysics, 1994.
(36) Poparić, G. B. Ph D. Thesis; University of Belgrade: Belgrade, Serbia, 2001.
(37) Kato, H.; Kawahara, H.; Hoshimo, M.; Tanaka, H.; Brunger, M. J.; Kim, Y. K. *J. Chem. Phys.* **2007**, *126* (6), 064307.
(38) Kawahara, H.; Kato, H.; Hoshino, M.; Tanaka, H.; Brunger, M. J. *Phys. Rev. A* **2008**, *77*, 012713.
(39) Mangan, M. A.; Lindsay, B. G.; Stebbings, R. F. *J. Phys. B: At. Mol. Phys.* **2000**, *33* (17), 3225–3234.
(40) Pitchford, L. C.; Oneil, S. V., Jr. *Phys. Rev. A* **1981**, *23* (1), 294–304.
(41) http://www.siglo-kinema.com/bolsig.htm.

JP8054922